

New Wholly-Aromatic Thermotropic Polyesters with Controlled Flexibility

Devdatt S. Nagvekar¹, Patrick T. Mather,^{2*} Hong G. Jeon,³ Loon-Seng Tan²

¹Univ. Dayton Research Inst., 300 College Park, Dayton, OH 45469

²AFRL/MLBP, 2941 P St., Wright Patterson Air Force Base, OH 45433

³Systran Corp., AFRL/MLBP, 2941 P St., Wright Patterson Air Force Base, OH 45433

Abstract

In this work, we present the synthesis and characterization of a new series of wholly-aromatic copolyesters derived from the condensation of various weight fractions of 4,4'-(*o*-phenylenedioxy)dibenzoic acid (OPDB) and substituted terephthalic acid (BTA) with 2-phenylhydroquinone (PHQ). The Higashi method, involving tosyl chloride and pyridine as solvent, was employed to yield polymer with significant molecular weight. These polymers are intended to enable accessible clearing transition *and* to control the balance of stiffness and toughness in melt-spun fibers systematically. We report the synthetic details along with characterization of quiescent phase behavior and morphology.

Introduction

Aromatic copolyesters which are para-linked are known to feature thermotropic behavior in which heating the semicrystalline solid results in melting to a mesomorphic phase, often nematic, giving rise to desirable molding characteristics, mechanical properties, and solvent resistance. Often, their high modulus and strength come at the expense of low toughness, manifested as failure strains less than 5%. In addition, such polymers feature nematic-isotropic transition temperatures in excess of thermal decomposition, eliminating the potential benefit of traversing the isotropic-nematic phase transition during processing.

Since thermotropic liquid crystallinity in polymers was first discovered in the 1970's, thermotropic LCPs have been predominantly aromatic polyesters. The two major commercial materials are wholly aromatic polyesters made from diacids (AA) and diols (BB), as well as from AB-type monomers, such as 2-hydroxy-6-naphthoic acid. These wholly-aromatic, para-linked, polyesters have found primarily as molding resins with mechanical properties approaching those of polymer matrix composites. In addition, fiber and film products are beginning to emerge.

Despite the success of thermotropic LCP technology, there are several significant challenges to be addressed. The first of these is the large disparity in mechanical properties between molding (30 ksi strength) and fiber spun (400 ksi strength) articles. Second is the extreme sensitivity of mechanical properties to the conditions of melt processing, such as extrusion speeds, temperature profile, and die design. We hypothesize that both of these problems can be addressed by designing LCPs characterized by accessible nematic-isotropic transition temperatures leading to two effects. First, the nematic defect history can be "erased" to obtain a reproducible starting morphology for processing. Second, the flow-induced isotropic-nematic transition¹ can be exploited to obtain outstanding orientational order and mechanical properties.

Previous approaches to lowering the nematic-isotropic clearing temperature have involved primarily the use of flexible spacers, as summarized in the review chapter by Sirigu.² Alternatively, the incorporation of non-linear, aromatic comonomers has enabled the reduction of nematic-isotropic clearing transition temperatures below the decomposition temperature. Many examples of the use of such monomers are given in the comprehensive review of Han and Bhowmik.³ Examples include such common monomers as isophthalic acid and resorcinol, as well as diaryl monomers, such as 3,4'-dihydroxybenzophenone. We have chosen an alternate

approach incorporating a triaryl-diether diacid that can adopt a range of conformations ranging, in principle, from a "straight" conformation to a bent conformation resembling a hairpin. Use of such a comonomer should enable an accessible nematic-isotropic transition temperature while still providing the ability to produce fibers and films of significant modulus and strength.

Experimental

Materials

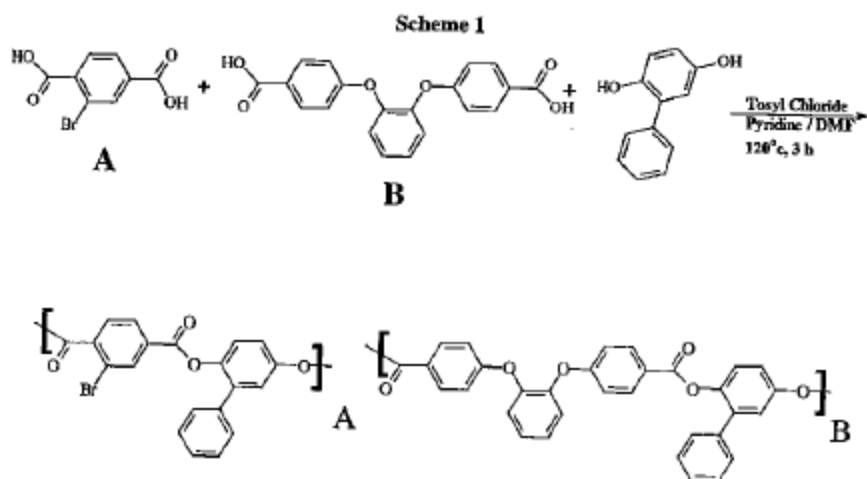
The monomers, 4,4'-(*o*-phenylenedioxy)dibenzoic acid (OPDB), 2-bromoterephthalic acid and phenyl hydroquinone were recrystallized at least three times from ethanol, acetic acid and chloroform, respectively. Anhydrous pyridine, dimethylformamide (DMF) were obtained from Aldrich and used without further purification. Tosyl chloride was recrystallized from hexane and dried in vacuum oven prior to its use.

Measurements

FTIR spectra were obtained using a Bruker IFS 28 FTIR spectrometer. The intrinsic viscosities were measured in an Ubbelohde viscometer thermostated at 30°C using *N,N*-dimethylacetamide (DMAc) as a solvent. Molecular weight data was determined using gel permeation chromatography (GPC) with DMAc as solvent and referencing polystyrene standards. Thermal analysis was conducted using a TA instruments differential scanning calorimeter with a heating rate of 30 °C/min to determine the glass transition temperature and the melting transition(s). Thermal decomposition was characterized using a TA Instruments thermal gravimetric analyzer with a heating rate of 10 °C/min. Polarizing optical microscopy was performed using a custom heating stage,⁴ along with an aus Jena polarizing microscope, a Panasonic KR222 CCD camera, and a Data Translations frame grabber. Wide angle x-ray scattering measurements were performed using a Rigaku rotating anode X-ray generator operated at 40kV and 250mA, using a *Cu* target and graphite monochromator. The specimens were mounted on pinhole collimator, and the diffraction patterns were recorded on a phosphoric image plate using a Statton camera.

Copolyester Synthesis (90:10 example)

As an example of the polymer synthesis, we describe the preparation of copolymer containing 90 mole percent of the 2-bromoterephthalic acid monomer and 10 mole percent of the flexible OPDB monomer. The procedure is shown schematically in **Scheme 1** below. A complete description of the monomer and polymer syntheses appears elsewhere.⁵ A solution of tosyl chloride (1.5011 g, 7.874 mmol), in pyridine (4 mL) and DMF (25 drops) was maintained at room temperature for 30 min and added to a mixture of 2-bromoterephthalic acid (0.6678 g, 2.725 mmol) containing OPDB (0.1061 g, 0.3029 mmol) in pyridine (2 mL). OPDB was prepared according to the literature.⁶ The mixture was maintained at room temperature for 10 min and then at 120°C for 10 min. To this solution was added dropwise over 15 min at 120°C phenylhydroquinone (0.5639 g, 3.028 mmol) in pyridine (6.5 mL). The reaction was maintained at 120°C for 3 h. The polymer, OPDB10, was isolated by precipitation with methanol. The precipitate was filtered and washed with methanol and dried. Purification was carried out first by dissolving the polymer in dimethylacetamide, filtering and precipitating into methanol. Vacuum oven drying at 75°C for 15 h gave pure polymer (1.23 g), 100% yield. IR (KBr, cm^{-1}): 1742, 1477, 1275, 1229, 1162, 1080, 1026, 896, 760, 737 and 698. $[\eta] = 0.710 \text{ g/dL}$. Anal. $\text{C}_{21.2}\text{H}_{11.9}\text{Br}_{0.9}\text{O}_{4.2}$: C 62.76, H 2.96, Br 17.72. Found C 62.53, H 2.74, Br 17.82.



Results and Discussion

The synthesis of wholly aromatic thermotropic polyesters (OPDBn; $n=0, 10, 20, 50, 100$) were carried out using a direct polycondensation method as reported by Higashi et al.^{7,8} Here, n refers to the mole percentage of the "B" repeat unit shown in Scheme 1. In this approach, the reaction takes place in pyridine and in the presence of tosyl chloride with DMF (catalytic amount), which forms *in situ* a Vilsmeier adduct and activates the diacid to produce mixed anhydride. Polycondensation of the anhydride and the diol led to the formation of the desired polyester. Fibrous homopolymers (OPDB0 and OPDB100) as well as copolymers (OPDB10, 20 and 50) were prepared in essentially quantitative yields as a result of this approach. The more rigid homopolymer, OPDB0, exhibited solubility only in DMAc, whereas the more flexible homopolymer OPDB100 was soluble in both DMAc and chloroform. Their intrinsic viscosity values range between 0.7 to 1.00 and 0.2 to 0.3 g/dL, respectively, depending on the polymerization conditions. We note that homopolymer OPDB0 was previously prepared from the melt transesterification of 2-phenylhydroquinone diacetate and 2-bromoterephthalic acid using 0.01% magnesium chloride as a catalyst, in which the resulting inherent viscosity was 0.85 dL/g (60/40 phenol/tetrachloroethane, 25°C, 0.5 g/dL).⁹

The compositions of the copolymers were in excellent agreement with the theoretical values with respect to the bromine contents. The fact that the feed ratio and the repeat unit ratio are practically the same suggests that despite the asymmetry in the molecular structure of 2-bromoterephthalic acid, both the diacid monomers used in the copolymerization are similar in their reactivities under Higashi reaction conditions. In our hands, reaction at 10% polymer concentration gave the highest weight average molecular weight and therefore, all other copolyesters were synthesized accordingly. The structures of polyesters were verified by IR spectroscopy, which showed characteristic absorption bands due to carbonyl and C-O-C stretch around 1740 and 1100 cm^{-1} , respectively. We summarize the solution characterizations of the OPDBn polymers in Table 1.

Thermal characterization of the OPDBn polymers, summarized in Table 2, revealed that the polymers all had modest glass transition temperatures, ranging from 108 °C to 138 °C, and

quite low melting points. The homopolymer OPDB0 features two weak melting transitions at $T = 190^\circ\text{C}$ and $T = 215^\circ\text{C}$, while OPDB10 and OPDB20 feature melting points of 230 and 232 $^\circ\text{C}$, respectively. The rest of the OPDBn polymers feature DSC traces free of any melting endotherm. These data, along with polarizing optical microscopy (POM) observations, indicate that the polymers OPDB50 and OPDB100 are purely amorphous thermoplastics. Of the polymers that were observed to possess a nematic liquid crystalline phase, only one (OPDB20) featured a nematic-isotropic clearing transition temperature below 400 $^\circ\text{C}$. For this polymer, POM observations revealed a clear loss of optical birefringence at $T = 375^\circ\text{C}$, at which temperature the sample transforms from a turbid nematic to a clear liquid appearing black between crossed polarizers.

The polymers were found to feature good thermal stability, as indicated in Table 2, marked by decomposition onset temperatures in the range of 450 $^\circ\text{C}$ to 490 $^\circ\text{C}$. We observed a slight improvement in the thermal decomposition temperatures with increasing OPDB percentage. The char yield (material remaining at $T = 900^\circ\text{C}$) was found to be independent of the polymer composition and was relatively high at 40%.

Table 1: Solution characterization of the OPDBn polymers. M_n and M_w data were measured relative to polystyrene standards using GPC. Solutions were prepared in DMAc.

| Composition | | | | M_n | M_w | M_w/M_n | $[\eta]$ g/dL |
|-------------|-----|-----------|------|-------|-------|-----------|---------------|
| Actual | | Observed* | | | | | |
| A | B | A | B | | | | |
| 1 | 0 | - | - | 13793 | 36739 | 2.66 | 0.958 |
| 0.9 | 0.1 | 0.91 | 0.09 | 12420 | 30791 | 2.56 | 0.710 |
| 0.8 | 0.2 | 0.81 | 0.19 | 10791 | 31237 | 2.89 | 0.759 |
| 0.5 | 0.5 | 0.51 | 0.49 | 5581 | 23958 | 4.29 | 0.489 |
| 0.0 | 1.0 | - | - | 11614 | 35342 | 3.04 | 0.330 |

* Composition was calculated from elemental analysis of bromine content in the polymer backbone.

Table 2: Thermal transitions for the copolyesters containing the specified mole percentages of the kinked repeat unit, B. Temperatures are in degrees celsius, T_{dec} is the temperature for 5% mass loss, and m_{ch} is percentage of initial mass remaining at 900 $^\circ\text{C}$.

| %B | T_g | T_{m1} | T_{m2} | T_{ni} | T_{dec} | m_{ch} |
|-----|-------|----------|----------|---------------|-----------|----------|
| 0 | 108 | 190 | 215 | -- | 463 | 37.3 |
| 10 | 129 | 230 | -- | -- | 454 | 40 |
| 20 | 133 | 232 | -- | -- (375, POM) | 459 | 41.8 |
| 50 | 138 | -- | -- | -- | 464 | 40.2 |
| 100 | 136 | -- | -- | -- | 493 | 39.6 |

Nematic textures of OPDB0, OPDB10, and OPDB20 were visible in the polarizing optical microscope (POM) when samples were prepared by casting from 1 wt. % solutions in DMAc solvent followed by vacuum drying and thermal annealing at $T = 250^\circ\text{C}$. Representative Schlieren textures for these samples are shown in Figure 1. We note that while these three polymers all show classic nematic ordering and textures, OPDB10 showed reproducibly a

nsitions at T
and 232 °C.
ny melting
ns, indicate
s. Of the
(OPDB20)
s polymer,
, at which
ring black

Table 2.
bserved a
g OPDB
endent of

red



of
ure

ve

"woven" type modification to the Schlieren texture (Figure 1, middle) that we have not found previously in the literature. This texture will be a subject of further study.

As-synthesized powder of the same polymers were prepared for POM by melting directly onto the glass plate of our custom heating stage, followed by squeezing with a cover slip or shearing with a heated razor. Using this procedure, we observe textures distinct from those observed for solution casting, as described above for Figure 1. Instead, we find banded textures immediately following shear, as has been reported for other systems,^{10,11} followed by quite uniform birefringence after long-time annealing. We have found that the tendency to form bands following shear followed the order OPDB0 < OPDB10 < OPDB20.



Figure 1. Polarizing optical micrographs showing the characteristic nematic texture for samples OPDB0, OPDB10, and OPDB20. The height of each micrograph is 35 microns.

Fibers drawn from the melt at 250 °C using the custom heating stage revealed significant orientation of the macromolecular chains, as indicated by concentration of the interchain spacing reflection on the equator, as shown in Figure 2 for OPDB0, OPDB20, and OPDB100. The level of orientation was found to be strongly dependent on the composition of the polymers, with OPDB0 featuring the highest orientational order ($\langle P_2 \rangle = 0.31$)¹² OPDB20 featuring an intermediate level of orientational order ($\langle P_2 \rangle = 0.18$) and OPDB50 featuring the lowest orientational order ($\langle P_2 \rangle = 0.06$). We note that the orientation data are quite sensitive to the conditions of melt drawing, which were not controlled rigorously. Moreover, we strongly believe that the level of orientation resulting from fiber processing will be a strong function of temperature, particularly above and below the nematic-isotropic transition temperature. Therefore, we do not draw the general conclusion that the level of orientation decreases with the amount of OPDB comonomer in the polymers. In addition to the concentration of the interchain spacing peak on the equator, the OPDB0 and OPDB20 show strong scattering on the meridian. Based on the POM experiments, we have not observed smectic phases in these polymers, thus we conclude that the meridian scattering corresponds to the repeat distance along the polymer chains within the nematic phase. The detailed study on phase transition and microstructure determination will be reported in a future publication.

Conclusions

Given our thermal, optical and microstructural observations, we are motivated to extend our studies to include other OPDBn copolymers which bridge the phase behavior spanned by OPDB20 ($T_m = 375$ °C) and OPDB50 (amorphous thermoplastic). It is expected that an intermediate composition exists which possesses a more desirable nematic-isotropic transition temperature (300 °C). Additionally, we plan to explore the role of the aromatic substitutions on both the terephthalic acid and hydroquinone phenyl rings in dictating the resulting phase behavior of the polymers. Once we have achieved the desired phase behavior in this wholly-

aromatic copolyester system, we intend to explore the processing of fibers and films in the vicinity of the nematic isotropic phase transition.

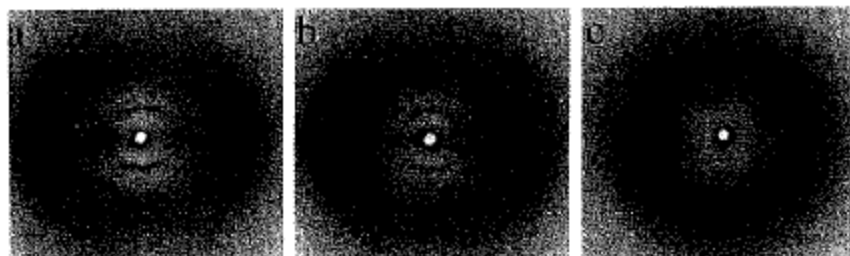


Figure 2. WAXS scattering patterns comparing the orientation of melt-drawn fibers of (a) OPDB0, (b) OPDB20, and (c) OPDB100 (right). The fiber drawing axis is along the vertical direction.

Acknowledgments

This work was supported by the Air Force Office of Scientific Research, Division of Chemistry and Life Sciences, and Air Force Research Laboratory, Materials and Manufacturing Directorate. Intrinsic viscosity data and GPC data were kindly provided by Rishi Bharadwaj and Charlie Benner, respectively.

1. P.T. Mather, A. Romo-Uribe, C.D. Han, S.S.Chang, *Macromolecules*, **30**, p. 7977 (1997).
2. In, "Liquid crystallinity in polymers : principles and fundamental properties," edited by Alberto Ciferri. New York : VCH Publishers, (1991).
3. H. Han and P.K. Bhowmik, *Prog. Polym. Sci.*, **22**, p. 1431 (1997).
4. P.T. Mather, H.R. Stüber, K.P. Chaffee, T.S. Haddad, A. Romo-Uribe, and J.D. Lichtenhan, *Mat. Res. Soc. Symp. Proc.*, **425**, p. 137 (1997).
5. D.S. Nagvekar, P.T. Mather, H.G. Jeon, and L.-S. Tan, *Manuscript in Preparation* (1999).
6. Tan, L.-S.; Venkatasubramanian, N., *J. Polym. Sci. Part A, Polym. Chem.*, **34**, p. 3539 (1996).
7. F. Higashi in "New Methods for Polymer Synthesis," ed. W. I. Mijs, Plenum Press, New York, pg.112 (1992).
8. F. Higashi, N. Akiyama, I. Takahashi, and T. Koyama, *J. Polym. Sci. A: Polym Chem. Ed.*, **22**, p. 1653 (1984).
9. W.R. Krigbaum, H. Hakemi, and R. Kotek, *Macromolecules*, **18**, p. 965 (1985).
10. M.G. Dobb, D.J. Johnson, B.P. Saville, *J. Polym. Sci.: Polym. Phys. Ed.*, **15**, p. 2201 (1977).
11. C. Viney, A.M. Donald, A.H. Windle, *J. Mater. Sci.*, **18**, p. 1136 (1983).
12. The orientation parameter, $\langle P2 \rangle$, is measured by azimuthal scanning of the primary reflection and subsequent numerical analysis following, e.g., W. Haase, Z.X. Fan, and H.J. Müller, *J. Chem. Phys.* **89**, p. 3317 (1988).